

Measurements of photoinduced refractive index changes in bacteriorhodopsin films

RAVINDER KUMAR BANYAL and B RAGHAVENDRA PRASAD

Indian Institute of Astrophysics, Sarjapur Road, Koramangala, Bangalore 560 034, India

E-mail: brp@iiap.res.in

MS received 12 December 2005; revised 6 November 2006; accepted 4 December 2006

Abstract. We report the pump–probe measurements of nonlinear refractive index changes in photochromic bacteriorhodopsin films. The photoinduced absorption is caused by pump beam at 532 nm and the accompanying refractive index changes are studied using a probe beam at 633 nm. The proposed technique is based on a convenient and accurate determination of optical path difference using digital interferometry-based local fringe shift. The results are presented for the wild-type as well as genetically modified D96N variant of the bacteriorhodopsin.

Keywords. Bacteriorhodopsin; refractive index change.

PACS Nos 42.65.-k; 78.20.-e; 07.60.Ly

1. Introduction

Bacteriorhodopsin (BR) is a photochromic protein extracted from the purple membrane of the bacterium (*Halobacterium salinarum*) found in saline environment. The molecule has received a considerable attention in recent years due to its unique and desirable optical properties [1,2]. A primary photocycle is initiated when the molecule in the ground state (B) that has a broad absorption band around 570 nm, absorbs a photon and passes through several structural transformation changes called intermediates. These intermediates, labeled J, K, L, M, N and O, are characterized by different lifetimes and distinct absorption spectrum in visible region. During the photocycle, each state can either thermally relax to next intermediate or can be switched directly back to B state if photoactivated by light of suitable wavelength that falls within its absorption band. BR also exhibits a strong nonlinear behaviour at very low laser powers. Several practical applications have been envisaged and successfully demonstrated by utilizing nonlinear absorption and refractive index changes (RIC) in BR. The spectral dependence between absorption and RIC can be described by the Kramers–Kronig relations. Moreover, the optical and dynamical properties of the BR can be modified genetically to suit a specific application.

In the past, researchers have used several methods to investigate the nonlinear properties of the BR films [3–8]. The Z-scan measurement is a simple experimental procedure that gives information about the optical nonlinearities of materials. A converging lens focuses the symmetric Gaussian beam through the film placed near the beam waist. Due to the ‘lensing effect’, the measured transmittance varies from peak to valley as the film is moved from one side of the beam waist to another. The nonlinear refractive index can be derived from the difference in power from the peak to the valley. The accuracy of Z-scan method is compromised due to finite absorption of light by the film sample and the non-Gaussian profile of the input beam [7,8].

Interferometric techniques have also been developed for measuring the small changes in refractive index of the materials in which the optical path difference (OPD) between two interfering light beams is inferred either by monitoring the intensity change with photodiode or by measuring the displacement in the fringe pattern recorded using a photographic plate or a CCD camera [6,9]. In either case, the OPD is computed from the data acquired at different times, that is, *before* and *after* the sample under investigation is subjected to external excitations that modify the optical path in one of the arms. Meanwhile in the intervening time, the OPD can also change due to the random phase fluctuations arising from mechanical vibrations and/or air turbulence. The commercially available anti-vibration platforms are susceptible to the low-frequency perturbations that can easily couple into the experiment. For example, we found that the fringe pattern remains stable only up to $\lambda/8$ when observed over a moderate period of time (>1 s). This feature implies the necessity of highly stable, well-isolated and vibration-free environment, where the phase fluctuations in the optical beam caused by external factors are much smaller than the expected phase change due to RIC in the tested object. These experiments require additional and often complex techniques to mitigate the effects of noise due to environmental instability.

In addition to a small but finite absorption of the probe beam by the BR sample, the accuracy of intensity-based interferometric measurements is further limited by power stability of the laser source.

In this article, we describe a Mach–Zehnder interferometer lay-out in conjunction with a pump–probe technique suitable for measuring the nonlinear index variations. As explained in the next section, the novelty of the proposed method lies in its immunity against random phase fluctuations while measuring the optical path difference. The ground-state density of the BR molecules is affected by the pump beam absorption at 532 nm and the accompanying RIC due to population redistribution of the molecules is measured using a weak probe beam at 633 nm. As stated before, using interferometry, the phase shift due to RIC of the material can be determined either by measuring the intensity change in the fringe pattern or by measuring the fringe displacement. However, owing to the broad band absorption of the ground state, BR also has a finite but small absorption (see figure 1) at 633 nm. To eliminate the effect of finite absorption in intensity-based measurements of the fringe pattern is not straightforward always [9]. Therefore, it is advantageous to use fringe shift technique that is immune to the probe beam absorption at 633 nm.

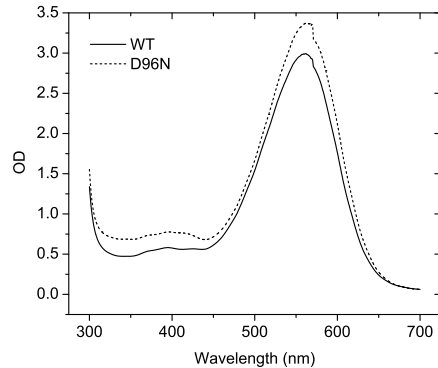


Figure 1. Spectral curves for wild-type and D96N films.

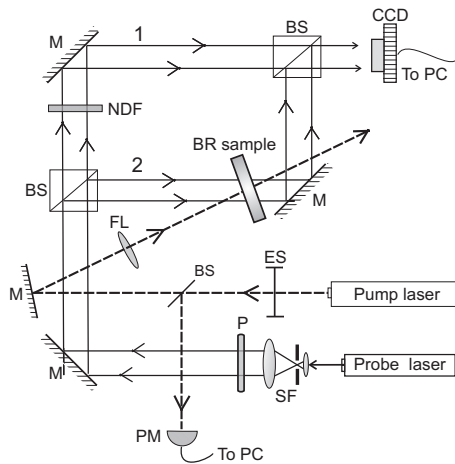


Figure 2. Experimental lay-out for measuring RIC. SF, spatial filter with beam expander; P, polarizer; PM, power meter; M, mirror; ES, electronic shutter; FL, focusing lens; BS, beam splitter; NDF, neutral density filter; CCD, charge coupled device.

2. Experiment

Experimental arrangement for measuring RIC is shown in figure 2. An expanded plane parallel beam from He-Ne laser ($\lambda = 633 \text{ nm}$) uniformly illuminates the entire BR sample placed in one of the arms of Mach-Zehnder interferometer. The beam intensity ($I \approx 50 \mu\text{W cm}^{-2}$) was well below the observed saturation intensity of the BR at 633 nm [8,10]. The set-up is adjusted to form straight line fringes that were aligned parallel to the lab vertical. As shown in figure 2, a small central region ($\approx 1 \text{ mm}^2$) of the BR sample is excited by a nearly focused and vertically polarized pump beam from diode-pumped Nd : YAG laser at 532 nm. The pump beam had a transverse Gaussian profile with $M^2 < 1.1$. For the two beams (1 and 2) with intensity I_1 and I_2 , the output intensity from the interferometer can be written as

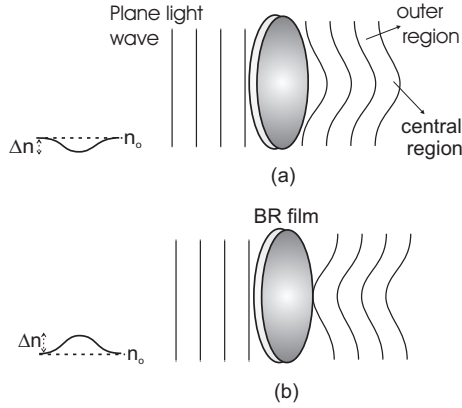


Figure 3. Illustration of wave-front modulation in response to RIC for (a) $-\Delta n$ and (b) $+\Delta n$.

$$I = I_1 + I_2 + 2\sqrt{I_1 I_2} \cos [(2\pi/\lambda)(n_0 r_1 - n r_2) + (\phi_1 - \phi_2)], \quad (1)$$

where ϕ_1 and ϕ_2 are the initial phases, λ is the light wavelength, and n is the intensity-dependent refractive index which is given by

$$n = n_0 + n_2 I_p. \quad (2)$$

Here, n_0 is the linear refractive index, n_2 is the nonlinear refractive index coefficient, and I_p is the intensity of the control or pump beam.

The ratio of pump to probe beam size on the film is very small. So the RIC is confined only within a small central portion of the BR film that is irradiated by pump beam. Accordingly, the optical path change in beam 2 occurs only along its central region, whereas the outer region remains unaffected. Depending on the sign of Δn , the phase front of the central region is either advanced or delayed. This is illustrated in figure 3. For clarity, the drawing in figure 3 is somewhat exaggerated. The effect of external vibrations would now be common to both the regions. Upon interference with beam 2, the modulated phase front of beam 1, causes a local fringe shift to appear in the middle part of the main interferogram. This local fringe shift persists and remains frozen on the randomly moving interferogram (caused by random phase fluctuations between beam 1 and beam 2) as long as the pump beam remains on. Therefore, in order to measure the fringe shift and hence OPD in the present set-up, it is not necessary (e.g. in ref. [6]) to capture the fringe pattern separately *before* and *after* the pump illumination. A single frame captured by CCD is sufficient to calculate the fringe shift. As a result, the error due to mechanical instabilities in the measurement of OPD has been eliminated to a great extent.

3. Result and discussion

The two types of BR films, namely wild-type (WT) and D96N films, used in our experiment were purchased from MIB (Munich Innovative Biomaterials GmbH,

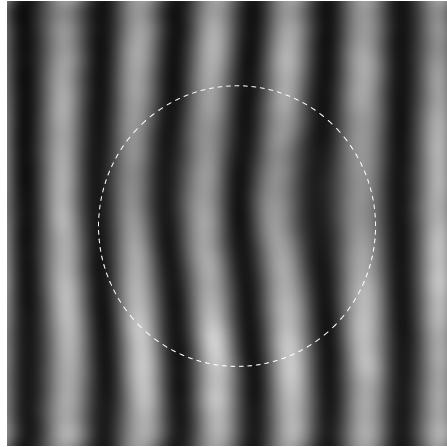


Figure 4. A processed CCD image of interferogram showing fringe distortion within the pump illuminated region.

Marberg, Germany). These circular films of diameter ≈ 19 mm, are sandwiched between high-quality optical glass (BK7 windows) which is permanently mounted in a rugged metal holder. The optical densities of the films are 3 (OD3) and 5 (OD5) at 570 nm. The films are neutral in pH (pH=7) and mainly contain gelatine plus some proprietary ingredients in smaller concentrations [11]. In response to photoinduced RIC in the pump irradiated region, a corresponding change in the optical path of the probe beam 2 results in a local shift or bending of interference fringes. Figure 4 shows the CCD (Pulnix TM-1320-15CL; number of pixels: 1300×1030 ; pixel size: $6.7 \times 6.7 \mu\text{m}$) image of the modified interferogram in the presence of pump beam.

The OPD can be easily found by measuring the curvature or the deviation of the affected fringes from the straight line. To improve the accuracy of the measurements, only five to six fringes were recorded on the entire CCD array. High-frequency fringing effect due to coherent illumination of CCD was removed by low-pass Fourier filtering of the image data. For further analysis, the gray scale images were converted into binary images using appropriate intensity threshold. The refractive index change Δn can be calculated using the expression

$$\Delta n = \frac{\lambda \Delta s}{d}, \quad (3)$$

where λ is the wavelength of the light, d is the film thickness and Δs is the fractional fringe shift measured in number of CCD pixels. Figure 5 shows the measured RIC and its nonlinear dependency on pump beam intensity for wild-type and D96N variant of BR films. A sigmoidal function was used to fit the experimental data. In all cases, the computed correlation coefficient r^2 between sigmoidal curve and measured data was found to be >0.98 .

The thickness of the film samples was $100 \pm 10 \mu\text{m}$. Due to the axial symmetry of the beams, the sign of the RIC cannot be inferred directly from the interferometric measurements. However, it is well-known from the Kramers–Kronig relations that the magnitude of the change in the real part of the refractive index increases as the

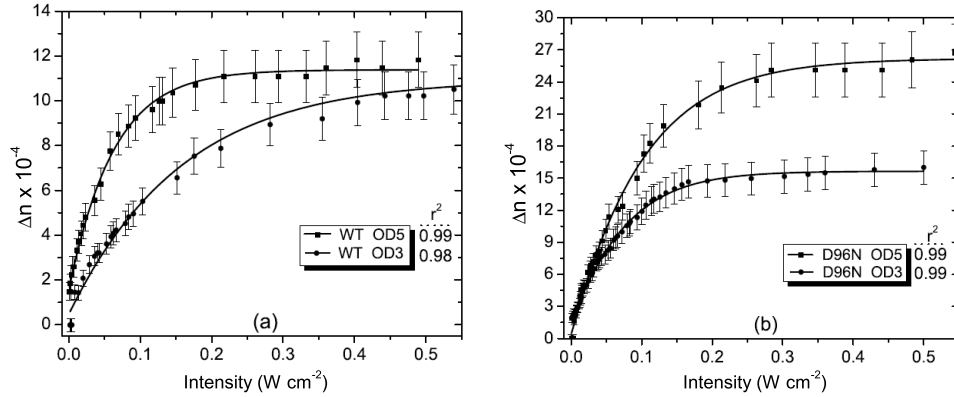


Figure 5. Photoinduced refractive index change vs. pump beam intensity for (a) the wild-type and (b) the D96N variant of BR film. The symbols are experimental data points and solid curves are sigmoidal fit to the measured data.

band-edge is approached from the higher wavelength side, thus rendering RIC positive [12]. Moreover, the refractive index at near-resonance wavelengths is minimum. Therefore, we did not observe any noticeable fringe shift when the experiment was repeated at 543 nm probe that had a significant ground-state absorption. The RIC ($\Delta n \approx 10^{-4}$) reported in refs [7,13] using Z-scan and phase-modulated techniques, is in close conformity with our results.

4. Error estimation

The quantities Δs and d in eq. (3) are not correlated and so the errors in their measurements can be reasonably treated as random and independent [14]. The error estimation in RIC, therefore, can be calculated using

$$\begin{aligned} \delta(\Delta n) &= \pm \lambda \sqrt{\left(\frac{1}{d} \delta(\Delta s)\right)^2 + \left(\frac{\Delta s}{d^2} \delta d\right)^2} \\ &= \pm \frac{\lambda}{d} \sqrt{\delta(\Delta s)^2 + \left(\frac{\Delta s}{d} \delta d\right)^2}. \end{aligned} \quad (4)$$

Here, $\delta(\Delta s) = 1/(\text{number of CCD pixels in one wavelength})$. From eq. (4), we note that the accuracy of determination of RIC depends more critically on the accuracy of the film thickness d . In the present case, we have not measured the film thickness independently, but relied on the value specified by the manufacturer. The stated uncertainty in the film thickness was $\delta d = \pm 10 \mu\text{m}$. In fact, the large error bars in figure 5 are due mainly to large uncertainty in the film thickness. Reducing the thickness uncertainty to half of its present value would cause nearly 50% reduction in $\delta(\Delta n)$. On the other hand, there will only be a minor improvement ($< 1\%$) if we could double the CCD resolution, say, by reducing the pixel size to half.

Additionally, thermal effect can also alter the refractive index due to the local heating of film by the pump beam. However, the thermal response of the BR films is usually an order of magnitude slower than the index change due to population redistribution. Therefore, to minimize the effect of heating, each interferogram image was recorded immediately (<2 s) after the pump beam was turned on.

5. Conclusion

In conclusion, we have presented a modified Mach–Zehnder interferometry-based pump–probe technique to determine the RIC in WT and D96N BR films. Refractive index change measured using a weak probe at 633 nm is shown to be induced by the the ground state excitation of BR molecules at 532 nm. The improved accuracy of the measurement is due to its immunity against errors that may arise from random phase fluctuations and finite probe beam absorption. The RIC was found to demonstrate saturation with increased pump intensity. In general, this technique can easily be implemented to carry out similar studies in photorefractive crystals, polymer films or any other transparent bulk materials.

References

- [1] N Hampp, *Chem. Rev.* **100**, 1755 (2000)
- [2] R R Birge, N B Gillespie, E W Izaguirre, A Kusnetzow, A F Lawrence, D Singh, Q W Song, E Schmidt, J A Stuart, S Seetharaman and K J Wise, *J. Phys. Chem.* **B103**, 10746 (1999)
- [3] O Werner, B Fischer and A Lewis, *Opt. Lett.* **17**, 241 (1992)
- [4] Z Yuan, Y Bao-Li, W Ying-Li, M Neimule, L Ming, C Guo-Fu and N Hampp, *Chin. Phys. Lett.* **20**, 671 (2003)
- [5] J Tallent, Q W Song, Z Li, J Staurt and R R Birge, *Opt. Lett.* **21**, 1339 (1996)
- [6] A Zeisel and N Hampp, *J. Phys. Chem.* **96**, 7788 (1992)
- [7] C Sifuentes, Y O Barmenkov and A V Kir'yanov, *Opt. Mat.* **19**, 433 (2002)
- [8] A V Kir'yanov, Y O Barmenkov, A N Starodumov, V-P Leppanen, J Vanhanen and T Jaaskelainen, *Opt. Commun.* **177**, 417 (2000)
- [9] V P Leppanen, T J Haring, T Jaaskelainen, E Vartiainen, S Parkkinen and J P S Parkkinen, *Opt. Commun.* **163**, 189 (1999)
- [10] F J Aranda, R Garimella, N F McCarthy, D Narayana Rao, D V G L N Rao, Z Chen, J A Akkara, D L Kaplan and J F Roach, *Appl. Phys. Lett.* **67**, 599 (1995)
- [11] M Wolperdinger, *An e-mail correspondence with MIB GmbH, Germany*, Aug. 24, 2005
- [12] J D Jackson, *Classical electrodynamics*, 3rd edn (Wiley, New York, 1998)
- [13] Y O Barmenkov, A V Kir'yanov, A N Starodumov, N M Kozhevnikov and H Lemmetyinen, *Appl. Phys. Lett.* **76**, 1801 (2000)
- [14] John R Taylor, *An introduction to error analysis*, 2nd edn (University Science Books, New York, 1996) Ch. 3